IOPscience iopscience.iop.org

Home Search Collections Journals About Contact us My IOPscience

Characterization of titanium nitride layers by positron annihilation and X-ray diffraction

This article has been downloaded from IOPscience. Please scroll down to see the full text article.

1994 J. Phys.: Condens. Matter 6 2943

(http://iopscience.iop.org/0953-8984/6/15/016)

View the table of contents for this issue, or go to the journal homepage for more

Download details:
IP Address: 171.66.16.147
The article was downloaded on 12/05/2010 at 18:11

Please note that terms and conditions apply.

J. Phys.: Condens. Matter 6 (1994) 2943–2948. Printed in the UK

Characterization of titanium nitride layers by positron annihilation and x-ray diffraction

K Uhlmann†, M Härting‡ and D T Britton†

† Universität der Bundeswehr München, Institut für Nukleare Festkörperphysik, D-85577 Neubiberg, Germany

‡ Universität der Bundeswehr München, BauV I/1 Physik, D-85577 Neubiberg, Germany

Received 26 November 1993, in final form 21 January 1994

Abstract. The two complementary techniques of positron lifetime spectroscopy and x-ray diffraction have been applied to the structural characterization of commercial titanium nitride hard coatings grown by hollow cathode arc evaporation. Use of a pulsed positron beam allows the layers to be analysed more or less independently of the substrate. The layers are found to consist of a single δ-phase TiN, with pronounced texture and residual stress. The dominant defects appear to be grain boundaries with a positron lifetime of 225 ps. Values for the bulk positron lifetime and diffusion coefficient are also obtained.

1. Introduction

Titanium nitride layers have sustained a wide interest for the last two decades [1], mainly because of their many possible applications, ranging from the purely decorative to industrial hard coatings. Recently TiN has found use in other areas, both as a diffusion barrier in silicon [2] and other structures [3] and because of its high infra-red reflectance [4].

The physical properties of the layers depend strongly on the structure, and therefore on the growth conditions, and can lie within a very broad range. For example the hardness can vary between 3 and 40 N mm^{-2} [1,5] and the electrical resistivity from 20 to 10 000 $\mu\Omega$ cm [1]. For a reliable technical application one has to assume the worst possible properties. Clearly, a better understanding of the layer formation process and characterization of the layers are of extreme technical and commercial importance.

TiN exists predominantly in two phases, δ-TiN and ε-Ti_2N [7]. The δ-phase has a sodium chloride structure with a stoichiometric lattice parameter of 0.4240 nm [6]. It is, however, stable over a relatively wide range of compositions from $TiN_{0.7}$ to $TiN_{1.16}$. Non-stoichiometric TiN contains vacancies in either the metal or metalloid sublattice, causing the lattice to relax into a configuration with a slightly reduced lattice parameter. Other effects associated with the growth process [1], e.g. thermal stress, substitutional oxygen and carbon, incorporated argon and interstitial nitrogen, can have a greater influence on the measured lattice parameter. Additionally, the growth conditions have a strong influence on other properties such as grain size (typically less than 100 nm), texture and the presence of the ε-phase and of voids [1,7,8].

In this paper, positron lifetime spectroscopy and x-ray diffraction have been applied to characterize commercially produced TiN layers. The two techniques are complementary, allowing a more complete characterization than with a single technique. X-ray diffraction probes the crystal structure of the layers, also yielding information on the composition and

0953-8984/94/152943+06$19.50 © 1994 IOP Publishing Ltd

stoichiometry, whereas positron annihilation is sensitive to the concentration and type of open volume defects. Although x-ray methods have been widely applied to the study of TiN layers [6, 9–12], positrons have rarely been used. Previous positron lifetime studies [12] have been limited by the bulk nature of the conventional technique, causing the signal from the layers to be swamped by that from the substrate. In this work, the layers have been studied with the Munich pulsed low-energy positron beam [13]. This is the first of only two time-resolved slow-positron beams worldwide, the other being in Japan [14].

2. Experimental details

The layers studied were produced, by Vakuumtechnik Dresden GmbH, by hollow cathode arc evaporation [15] of titanium in an argon–nitrogen plasma onto mild steel substrates. The exact growth conditions are not available, but the samples can be divided into two groups (designated as types I and II) corresponding to different N_2 partial pressures. All layers of each type were produced in the same batch, with different layer thicknesses obtained by placing the substrates at different positions with respect to the evaporator. The thicknesses of the layers were estimated by the manufacturer using x-ray fluorescence.

The positron annihilation measurements were carried out at ambient temperature using the Munich pulsed positron beam. Positrons from a 500 MBq ^{22}Na source are moderated in a 1 μm tungsten foil and a small fraction ($\sim 10^{-4}$) diffuse to the exit surface. These are then guided by a longitudinal magnetic field to the target, where they are accelerated to the required incident energy. The timing signal required for the lifetime spectrometer is obtained by pulsing the beam at 200 MHz. During the measurement the coincidence count rate in the spectrum was approximately 40 cps, depending on the incident energy with a time resolution of 185 ps FWHM. The total number of counts in each spectrum was typically 5×10^5.

Initially all the spectra were analysed in a conventional manner, assuming exponential lifetime components from which the mean lifetime was calculated from a fit to two components. In the near-surface region this is not strictly correct as spatial diffusion of the positron is not taken into account [16]. Nevertheless this treatment gives useful semi-quantitive information regarding the nature of any defects present and the diffusion back to the surface.

Two of the thicker layers, one of each type, 2.3 μm and 2.4 μm thick respectively, were studied in more detail with x-ray diffraction and with a more detailed analysis of the positron annihilation spectra taking spatial diffusion into account [17]. The diffraction measurements were performed in Bragg–Brentano geometry using Cu Kα radiation at the crystal analysis laboratory of the Technical University of Munich. A conventional diffractometer, running at 40 kV/30 mA was used to scan a 2θ range from 20° to 120° in steps of 0.05°. The primary beam was apertured at 1.5 mm width and the secondary slits at 0.2 mm. Each step was measured for 30 min. To identify the substrate peaks, an uncoated piece of the same steel was also measured.

Positron annihilation spectra from the same two layers as studied by x-ray diffraction have been analysed in detail using a model describing the diffusion and annihilation of the positron. It is not feasible to apply the same procedure to the thinner layers where at almost all energies the substrate has a substantial contribution. In commercial coatings such as these the substrate is neither well prepared nor characterized. The evolution of the various positron states after thermalization in a solid is well described by a diffusion–annihilation equation [18], governing motion of the positron in the bulk, combined with

spatially dependent rate equations, which describe trapping and annihilation both at defects and the surface. In addition to the defect lifetimes and trapping rates required in a normal trapping model, both the positron diffusion coefficient and the surface boundary condition need to be included. Using a finite-difference algorithm the annihilation spectrum for a specific implantation energy, can be stepped through, picosecond by picosecond, until the full lifetime spectrum has been constructed. After convolution with the instrumental resolution, this can be compared with the measured spectrum. Although, in principle, each spectrum contains all the spatial information determining the history of the positron, the results for a single spectrum can be ambiguous. In particular the apparent diffusion coefficient is strongly influenced by the surface escape rate and, to a lesser extent, by the defect trapping rate. It is, therefore, necessary to analyse all the measured spectra together to obtain consistent results.

3. Results and discussion

The diffraction patterns for the two different layers are shown in figure 1 with the TiN peaks marked. These have been identified according to [9]; the unmarked peaks result from the steel substrate. Several differences between the two samples are apparent. Firstly, in the type II sample, there is a clear signal from an α-Ti buffer layer between the substrate and nitride layer. This is not present in the type I sample. However, in neither layer is there any evidence of the ε-Ti_2N phase. Secondly the intensities of the δ-TiN (111) and (222) peaks compared to the (311) peak are different in the two samples, indicating pronounced texture.

Table 1. The lattice parameters of the different δ-TiN diffraction peaks for the two types of layer.

	Lattice parameter (nm)	
hkl	Type I	Type II
222	0.4285	0.4282
311	0.4273	0.4263
220	0.4279	0.4258
200	0.4250	0.4247
111	0.4282	0.4289
Mean	0.4274(13)	0.4269(15)

The lattice parameters for the different δ-phase reflexions are given in table 1. Within the experimental accuracy the mean lattice parameter is the same in both types and corresponds to that of stoichiometric TiN [6]. However, the lattice parameters are different for different directions indicating a complex stress state in the layers. This is greater in the type II layer, which has the intermediate Ti layer. A detailed analysis is beyond the scope of these measurements, although the depth dependent stress state could be achieved with a suitable modification of the method given in [19]. This would, however, require considerably more measurements at a much higher resolution.

The mean positron lifetimes are shown in figure 2 as a function of incident positron energy for all the layers studied. Qualitatively, all the layers are similar with a mean positron lifetime in the range of 220–225 ps. The limiting low-incident-energy lifetime between 300

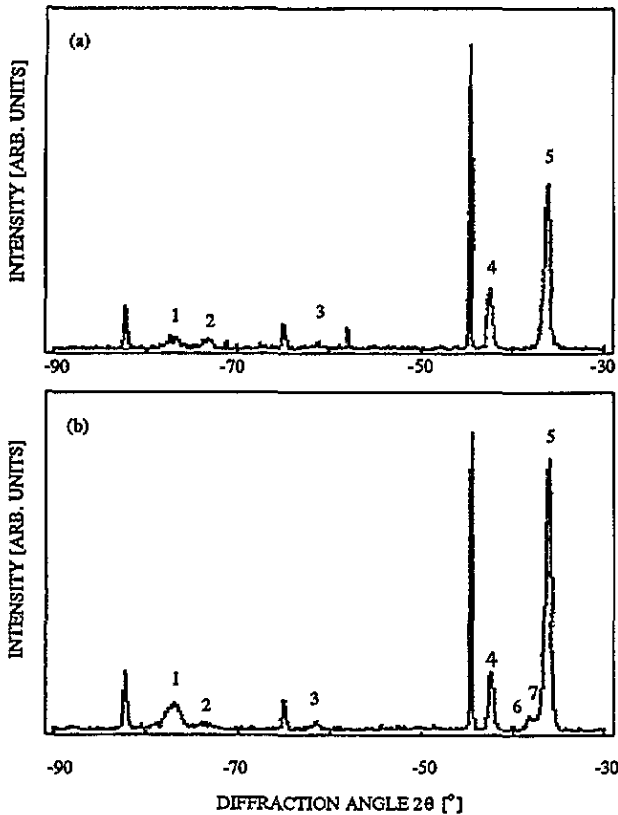

Figure 1. A selected region from the diffraction patterns for the two different layers, (a) type I, 2.4 μm and (b) type II, 2.3 μm, showing the TiN peaks. The respective peaks are 1, δ-TiN (222); 2, δ-TiN (311); 3, δ-TiN (220); 4, δ-TiN (200); 5, δ-TiN (111); 6, α-Ti (011) and 7, α-Ti (002).

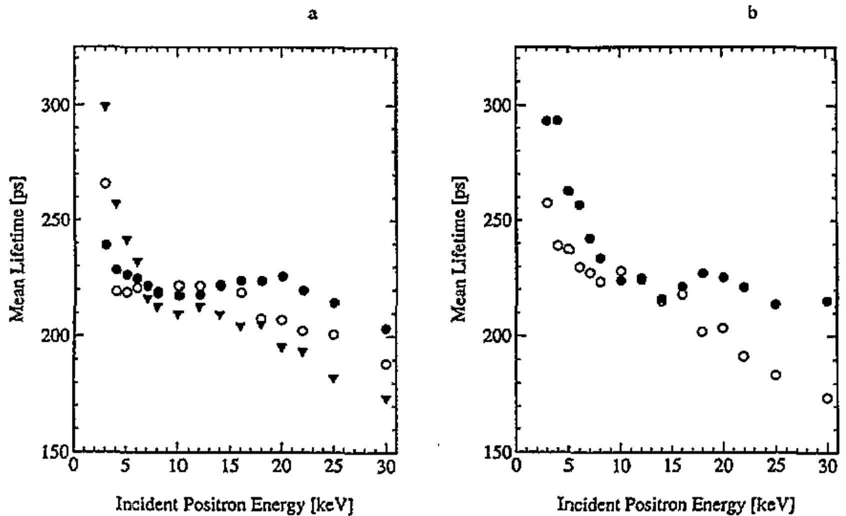

Figure 2. The mean lifetime as a function of incident positron energy: (a) type I, 1.21 μm (○), 1.4 μm (▼) and 2.4 μm (●); (b) type II, 1.03 μm (○) and 2.3 μm (●).

and 400 ps is typical of a 'dirty' surface [17, 20, 21] and yields no information about the clean TiN–vacuum interface. However, the sharp fall-off of the mean lifetime in the type I

layers is indicative of virtually no diffusion of thermal positrons to the surface, whereas the type II layers exhibit an almost continual change from the surface lifetime to that of the substrate. Below 8 keV incident energy, which corresponds to a mean implantation depth of 200 nm [22], a significant fraction of positrons reaches the surface before attaining thermal equilibrium [17, 23]. At present there is no way of including these in the analysis.

The reduction in surface signal in the type I layers could have several causes: either reduced diffusion, either due to trapping or a change in diffusion coefficient, or a change in the surface potential barrier preventing positrons penetrating the surface. To obtain further information, the two thicker layers of each type were analysed using the diffusion model described above in the incident energy range 8–14 keV, where contributions due to epithermal positrons and the substrate can be neglected.

Table 2. Positron diffusion and annihilation parameters for the two thicker layers.

	Type I	Type II
Bulk lifetime (ps)	170(5)	170(5)
Surface lifetime (ps)	370(30)	370(15)
Defect lifetime (ps)	225(3)	226(4)
Diffusion coefficient ($cm^2\ s^{-1}$)	1.30(20)	1.35(15)
Trapping rate (GHz)	5.1(3)	3.2(3)

Consistent results were obtained for both layers, with only a change in trapping rate (table 2). The annihilation and diffusion parameters were first determined for the type I layer so that values were approximately constant throughout the incident energy range studied. The parameters were then varied around these values for the type II layer, with most variation allowed for the defect lifetime and trapping rate. The diffusion coefficient and bulk lifetime are properties of the positron in the perfect lattice, and should therefore be similar in both samples. The defect lifetime and trapping rate, however, represent the defect structure in the sample and can differ widely between the two samples. Attempts to force the trapping rate in the type II layer to that in the type I resulted in values for the other parameters, particularly the diffusion coefficient, that varied throughout the incident energy range.

Both layers contain the same dominant defect with a positron lifetime of 225 ps and have the same bulk lifetime of 170 ps. The latter is, to our knowledge, the first reliable measurement of the bulk positron lifetime in δ-TiN. The defect lifetime of 225 ps is somewhat too short to correspond to positrons trapped at single vacancies. Although the vacancy lifetime is not known from the literature, as these layers are metallic, a value typically 50% longer than the bulk lifetime should be expected. This is however, only a very rough guide, but is applicable to pure Ti and its alloys. Recently published results for Ti [24] indicate a vacancy lifetime of 250 ps compared to a bulk lifetime of around 150 ps. In the same study, a shorter defect lifetime of 210 ps in low-temperature-deformed Ti is attributed to a mixture of defect types including dislocations.

The 225 ps component could probably be due to trapping at grain boundaries, which have a smaller free volume than vacancies, with the difference in trapping rate suggesting that the grain size is slightly larger in the type II sample. There is no evidence of longer-lived components, corresponding to a significant concentration of vacancies or voids, in agreement with the x-ray result that the composition of these layers is (very nearly) stoichiometric.

4. Conclusions

The two techniques used give complementary information, allowing a better structural characterization of the samples than with a single technique. X-ray diffraction shows the layers to be single δ-TiN phase, except for the present of an intermediate α-Ti buffer layer in the type II samples. The dominant defect has a partial vacancy character and can be attributed to grain boundaries. The difference in trapping rate between the two types of layer is probably due to differences in the grain size, with type II layers having, on average, slightly larger grains. There is no evidence of a significant concentration of vacancies or larger defects, suggesting that the layers are stoichiometric. This is confirmed by the measurement of the lattice parameter by x-ray diffraction. Diffraction measurements also indicate pronounced texture and residual stress in the layers, with the type II layers being more stressed than those of type I. Finally, we have obtained the first measurements of the bulk positron lifetime and positron diffusion coefficient in TiN.

References

[1] Sundgren J-E 1985 *Thin Solid Films* **128** 21

[2] Grigorov K G, Grigorov G I, Stoyanova M, Vignes J-L, Langeron J-P and Denjean P 1992 *Appl. Phys.* A **55** 502

[3] Weiser P S, Prawer S, Hoffman A, Manory R R, Paterson P J K and Stuart S-A 1992 *J. Appl. Phys.* **72** 4643

[4] Bonelli M, Guzman L A, Miotello A, Calliari L, Elena M and Ossi P M 1992 *Vacuum* **43** 459

[5] Wulff H, Basner R and Lunk A 1988 *Proc. 9th Conf. on High Vacuum, Interfaces and Thin Films* (Dresden: Physikalische Gesellschaft der DDR) p 372

[6] Sundgren J-E, Johansson B-O, Karlsson S-E and Hentzell H T G 1983 *Thin Solid Films* **105** 367

[7] Fair J A and Delfino M 1991 *Appl. Surf. Sci.* **53** 206

[8] Thornton J A 1986 *J. Vac. Sci. Technol.* A **4** 3059

[9] Zhang N, Zhai W, Wang Y and Wagendristel A 1993 *Vacuum* **44** 51

[10] Quaeyhaegens C, Stals L M, van Stappen M and de Schepper L 1991 *Thin Solid Films* **197** 37

[11] Ai C F, Wu J Y and Lee C S 1993 *Vacuum* **44** 99

[12] Schaffer J P, Perry A J and Brunner J 1992 *J. Vac. Sci. Technol.* A **10** 193

[13] Schödlbauer D, Sperr P, Kögel G and Trifshäuser W 1988 *Nucl. Instrum. Methods* B **34** 258

[14] Suzuki R, Kobayashi Y, Mikado T, Ohgaki H, Chiwaki M, Yamakazi T and Tomimasu T 1991 *Japan. J. Appl. Phys.* **30** L532

[15] Fleischer W, Schulze D, Wilberg R, Lunk A and Schrade F 1979 *Thin Solid Films* **63** 347

[16] Britton D T 1991 *J. Phys.: Condens. Matter* **3** 681

[17] Britton D T 1994 *Proc. R. Soc.* A **444** at press

[18] Nieminen R M and Olivia J 1980 *Phys. Rev.* B **22** 2226

[19] Härting M and Fritsch G 1993 *J. Phys. D: Appl. Phys.* **26** 1814

[20] Britton D T, Willutzki P, Jackman T E and Mascher P 1992 *J. Phys.: Condens. Matter* **4** 8511

[21] Britton D T, Willutzki P, Trifshäuser W, Hammerl E, Hansch W and Eisele I 1994 *Appl. Phys.* A **58** at press

[22] Vehanen A, Saarinen K, Hautojärvi P and Huomo H 1987 *Phys. Rev.* B **35** 4606

[23] Huomo H, Vehanen H, Bentzon M D and Hautojärvi P 1987 *Phys. Rev.* B **35** 8252

[24] de Diego N, Serra A, Segers D, Dorikens-Vanpraet L and Dorikens M 1992 *Mater. Sci. Forum* **105–110** 949